

**A shift in western tropical Pacific sea-level trends during the
1990s**

MARK A. MERRIFIELD *

University of Hawaii, Honolulu, Hawaii

* *Corresponding author address:* Mark A. Merrifield, Department of Oceanography, University of Hawaii at Manoa, 1000 Pope Road, MSB 317, Honolulu, Hawaii, 96822.

E-mail: lmarkm@soest.hawaii.edu

ABSTRACT

Pacific sea surface height trends from satellite altimeter observations for 1993 to 2009 are examined in the context of longer tide gauge records and wind stress patterns. The dominant regional trends are high rates in the western tropical Pacific and minimal to negative rates in the eastern Pacific, particularly off North America. Interannual sea level variations associated with El Niño-Southern Oscillation events do not account for these trends. In the western tropical Pacific, tide gauge records indicate that the recent high rates represent a significant trend increase in the early 1990s relative to the preceding 40 years. This sea-level trend shift in the western Pacific corresponds to an intensification of the easterly trade winds across the tropical Pacific. The wind change appears to be distinct from climate variations centered in the North Pacific, such as the Pacific Decadal Oscillation. In the eastern Pacific, tide gauge records exhibit higher amplitude decadal fluctuations than in the western tropical Pacific, and the recent negative sea-level trends are indistinguishable from these fluctuations. The shifts in trade wind strength and western Pacific sea level rate resemble changes in dominant global modes of outgoing longwave radiation and sea surface temperature. It is speculated that the western Pacific sea level response indicates a general strengthening of the atmospheric circulation over the tropical Pacific since the early 1990s that has developed in concert with recent warming trends.

1. Introduction

Since 1993, global mean sea level has risen at a rate just over 3 mm yr^{-1} based on satellite altimeter sea surface height (SSH) observations (Bindoff et al. 2007). Departures from the global rate are substantial on regional scales, with the standard deviation of the trend (2.8 mm yr^{-1} for 1° gridded data in Fig. 1) nearly as large as the mean. Notable trend extrema in the Pacific Ocean include high positive rates ($\sim 10 \text{ mm yr}^{-1}$) in the western tropical Pacific (WTP), and negative rates in the eastern tropical Pacific (ETP) and northeast Pacific (NEP). In this study, a number of questions regarding regional Pacific sea-level trends are considered: Are the dominant sea-level trends associated with the timing and amplitude of interannual El Niño-Southern Oscillation (ENSO) events over the short 17-year record, or with longer time scale climate modes such as the Pacific Decadal Oscillation (PDO) (Mantua et al. 1996) or the North Pacific Gyre Oscillation (NPGO) (Di Lorenzo et al. 2008)? How are the sea level rates related to changes in wind forcing? Are trends in the tropics and the NEP linked, i.e., via atmospheric co-variations or oceanic wave adjustments?

High rates of sea-level rise in the WTP have been attributed to interannual variations in sea level, which dominate short-term sea-level trend estimates. For example, Church et al. (2006) combined tide gauge and altimeter data to produce a reconstruction of sea level variability in the tropical and sub-tropical Indo-Pacific for 1950 to 2001. From 1993 to 2001, the reconstruction indicates high rates of sea-level rise in the western Pacific, similar to Fig. 1. The authors concluded that the pattern reflects a shift from weak El Niño conditions early in the record to more La Niña conditions in 2001. Reconstructions for 1950 to 2001 do not show unusually high trends in the WTP, with rates close to the late twentieth century global

average. A number of model studies have reproduced the high observed WTP sea-level trend pattern for different sections of the satellite altimeter record (1992-2002 Köhl et al. (2007), 1993-2001 Lombard et al. (2009), 1993-2008 Timmermann et al. (2010)). These studies attribute high WTP rates in large part to the influence of recent ENSO events, particularly the energetic 1997-98 El Niño.

Decadal variations in WTP sea level have been examined by Lee and McPhaden (2008) for the period 1993 to 2006. Trade winds in the central equatorial Pacific increased from 1993 to 2000, leading to high water levels in the WTP and low levels in the ETP. The pattern reversed as winds diminished from 2000 to 2005. Feng et al. (2010) showed that the tendency for increased trades and high WTP water levels reestablished after 2005. They related the multi-decadal sea level variability in the WTP to a strengthening of the shallow meridional overturning circulation in the tropics since the early 1990s described by McPhaden and Zhang (2004). The period of increased trade winds followed a weakening trend since the late 1970s (McPhaden and Zhang 2002). Carton et al. (2005) attributed increasing sea level in the WTP during 1993 to 2001 to enhanced trade winds west of the dateline, as well as to a weakening of trade winds in the Indian Ocean. They further noted that changes in sea level in the WTP are associated with a basin-scale decadal fluctuation in thermocline depth, that resembles changes in the PDO index. Qiu and Chen (2010) found good agreement between modeled and observed interannual to decadal sea level fluctuations at Guam using a 1 1/2-half layer model forced by reanalysis wind stress.

Sea level variations in the WTP and along the eastern boundary of the Pacific (Figure 1) have been linked dynamically to tropical wind forcing via equatorial- and coastal-trapped wave propagation (Li and Clarke 1994; Clarke and Lebedev 1996). Regional wind forcing

also strongly influences NEP sea level (Chelton and Davis 1982; Lageroef 1997; Fu and Qiu 2002; Cummins and Freeland 2007), with decadal and interdecadal sea level variability linked to the PDO (Jevrejeva et al. 2006), the Pacific North American (PNA) Index (Firing et al. 2004), and the NPGO (Di Lorenzo et al. 2008). Di Lorenzo et al. (2008) also noted that correlations of the NPGO index with observed SSH and sea surface temperature (SST) suggest a dynamical coupling between the tropics and sub-tropics. In general, the relationship between wind forcing, climate modes, and Pacific sea level response on decadal and longer time scales is receiving more attention as the satellite altimeter SSH record lengthens.

In this study, sea level records from altimetry and tide gauges and reanalysis wind stress (section 2) are used to examine recent regional sea-level trends in the Pacific in relation to wind variations. Contrary to previous assessments based on shorter records, interannual ENSO events account for only a small fraction of the 1993 to 2009 sea-level trends in the tropical Pacific (section 3). Tide gauge records indicate that the current high sea-level trends in the WTP represent a significant shift in trend since the early 1990s compared to the previous 40 years (section 4). The recent low sea-level trends along the NEP boundary are indistinguishable from decadal sea level variations. Enhanced Pacific trade winds since the early 1990s are linked to the high sea-level rates in the WTP (section 5). The timing of the trade wind enhancement in the tropical Pacific coincides with changes in global SST and outgoing longwave radiation (OLR) modes, suggesting that WTP sea-level trend represents the wind-forced response to an enhancement of the atmospheric circulation over the Pacific Ocean since the early 1990s (section 6).

2. Data

Time series of monthly-averaged sea level from tide gauge stations were obtained from the Permanent Service for Mean Sea Level (Woodworth and Player 2003). These records were extended forward in time using Fast Delivery data from the University of Hawaii Sea Level Center. An inverse barometer adjustment to the sea level time series was not made as the correction is small compared to the signals of interest. The vertical datum of the sea level records is fixed relative to local benchmarks. No correction has been made for vertical land movement at the benchmarks.

The operator of the Guam tide gauge, the Center for Operational Oceanographic Products and Services (CO-OPS) National Oceanic and Atmospheric Administration (NOAA), notes that a change in sea-level trend occurs after the 1993 Guam Earthquake, which resulted in liquefaction of alluvium and fill in the port area where the tide gauge is located. The stability of the tide gauge datum for the post-earthquake record therefore is a concern and CO-OPS continues to monitor survey records from the site. At this time there is no independent indication of land stability problems in the Guam tide gauge that would explain the post-1993 trend change.

To examine sea level variability in the NEP, a subset of tide gauge records is selected from the numerous CO-OPS stations available along the west coast of North America. The tide gauge records at San Diego, San Francisco, Seattle, and Ketchikan are representative of other stations in the region. In the ETP, the Santa Cruz station provides the longest continuous island tide gauge record in the region. Central and South American coastal stations with longer records than Santa Cruz are not included because of suspicious level shifts, due in

part to seismic activity, that appear specific to individual stations and not representative of regional sea level change.

The European Centre for Medium-Range Weather Forecasts (ECMWF) operational ocean analysis/reanalysis system (ORA-S3) (Balmaseda et al. 2008) product is used to describe surface wind stress variability. The time series are from 1959 through 2009 on a $1^\circ \times 1^\circ$ grid. The sea surface height data were obtained from the multimission, gridded sea surface altimeter product produced by Ssalto/Duacs and distributed by Aviso. The Interpolated Outgoing Longwave Radiation(OLR) data were provided by the NOAA/OAR/ESRL PSD, Boulder, Colorado, USA from their Web site at <http://www.esrl.noaa.gov/psd/>. Optimum Interpolation Sea Surface Temperature (OISST) data were obtained from the NOAA Environmental Modeling Center, Global Climate and Weather Modeling Branch. International Comprehensive Ocean-Atmosphere Data Set (ICOADS) SST data were obtained from NOAA/OAR/ESRL/PSD at <http://icoads.noaa.gov/>. The Nino3 and PDO indices were obtained from the NOAA National Weather Service Climate Prediction Center, and the NPGO from the website (<http://www.o3d.org/npgo/>) maintained by E. Di Lorenzo.

The present analysis is based on five-year running means of annual-averaged time series. The low-pass filter is used to suppress interannual ENSO variability and to focus on interdecadal time scales of variability. Attempts were made to extract interannual ENSO signals using linear regression techniques. Because the main results of this study were not affected significantly by the extraction, a simple running mean filter is applied to all datasets unless indicated otherwise. For tide gauge time series that include gaps, a seasonal cycle is removed and the annual average computed if at least eight months of data are available for a given year. The five-year mean for any section of data is computed if at least four years of data

are available.

3. 1993-2009 sea-level trends and interannual ENSO variability

The contribution of ENSO variability to the 17-year sea-level trends depicted in Fig. 1 is assessed. The interannual ENSO component of annual average sea surface height is estimated using a multiple regression $\hat{\eta} = b_0 + b_1t + b_2N + b_3\tilde{N}$ that includes time (t), the annual average Nino3 index (N), and the Hilbert transform of the annual average Nino3 index (\tilde{N}). N is used to represent in-phase ENSO variability across the tropical Pacific, with \tilde{N} included to capture quadrature variability associated with propagating signals. The trends associated with ENSO (Fig. 2) are computed as $a_1 - b_1$, where a_1 is the trend from the linear regression $\hat{\eta} = a_0 + a_1t$.

The ENSO-related trends are confined largely to the tropical Pacific as expected (Fig. 2). High rates in the WTP and low rates in the upwelling region of the ETP suggest the influence of La Niña events late in the 17-year record as well as the strong El Niño event early in 1997-98. Although the spatial pattern in Fig. 2 resembles the 1993 to 2009 SSH trend signal in the tropics (Fig. 1), the ENSO-related rates are nearly an order of magnitude smaller than the peak SSH trends. The spread of ENSO anomalies along the coast in the NEP is evident in Fig. 2 primarily south of the Baja California peninsula. Similar results are obtained using the same multiple regression as above but with monthly-averaged data, \tilde{N} removed, and N time-shifted to give the maximum correlation with SSH at each grid

point. Thus, the ENSO-related trends are too small to account for the spatial pattern of 1993 to 2009 SSH trends along North America.

The regression results suggest that the trend extrema in Fig. 1 are not an artifact of the timing and amplitude of interannual ENSO events. Similar trends as depicted in Fig. 2 are obtained using the Multivariate ENSO Index, the Southern Oscillation Index, and the Nino3.4 index as a proxy for ENSO instead of Nino3. As noted by Chen et al. (2008), Compo and Sardeshmukh (2010) and others, limitations exist in identifying ENSO-related variations using regressions with ENSO indices. In addition, the use of a five-year running mean inevitably leads to leakage of interannual ENSO variability to lower frequencies, despite efforts to account for the interannual signal in a regression analysis. Nevertheless, it remains unlikely that interannual ENSO events account for the 1993 to 2009 high WTP-low NEP sea-level trends.

4. Sea level trends and tide gauge records

The tide gauge records at Guam and Kwajalein are the longest in the WTP trend hot spot region (Fig. 3), dating back to the mid-twentieth century. Five-year mean time series at these stations show sea-level trends during the satellite altimeter period that are much higher than prior to the 1990s (Fig. 4). The linear trends for the section of data prior to 1993 are -0.8 ± 0.8 and 1.0 ± 0.5 mm yr⁻¹ at Guam and Kwajalein, respectively, compared to 9.9 ± 3.1 and 7.8 ± 0.9 mm yr⁻¹ after 1993. The uncertainties here are twice the standard deviation of the trend based on a Monte Carlo analysis of red-noise synthetic data. Trend adjustments due to the inverse barometer effect are small for both stations (0.1-0.3 mm

yr⁻¹).

Other WTP tide gauge records exhibit considerable spatial variability (Fig. 5). A comparison to the SSH time series from the grid point nearest each tide gauge (thin curves in Fig. 5) confirms that the tide gauges measure similar sea-level trends and variability as the satellite altimeters. Malakal has experienced more decadal time-scale variations than Guam or Kwajalein, and a recent trend increase is less apparent given these fluctuations. Majuro is farther east from the trend maxima than Kwajalein (Fig. 3), and little indication of a trend increase exists at this location. South of the equator, a trend increase after 1990 is evident at Kapingamarangi, Nauru, Funafuti and to a lesser extent Honiara, where a sea level minimum occurs in the late 1980s to mid 1990s. Kanton is located well east of the high trend levels and more decadal variability exists at this location compared to the other sites. Pago Pago and Suva, the southernmost stations in the region, do not clearly show a trend increase in the 1990s. A large sea level change occurs in the 1980s at Suva.

An average of all WTP sea level time series pictured in Fig. 5 shows clearly the abrupt trend change in the early 1990s that appears in the Guam and Kwajalein records (Fig. 6). The average of the first difference in time of the annual sea level time series is computed, and then integrated to obtain mean WTP sea level. To ensure that the long records at Guam and Kwajalein are not dictating the trend change, the average is computed without these two records and also excluding Pago Pago. Despite the presence of decadal variability in the WTP time series (Fig. 5), the average of the short records still shows the clear change in rise rate in the early 1990s (Fig. 6). Based on the average of all stations (solid curve in Fig. 6), the trend rate is -0.5 ± 0.3 mm yr⁻¹ prior to 1993 compared to 6.9 ± 1.6 mm yr⁻¹ after 1993.

In the eastern Pacific, decadal sea level variations tend to be larger in amplitude and more similar between tide gauge stations than in the WTP (Fig. 7). The correspondence between the tide gauge and satellite altimeter time series variations is poorer than in the WTP, presumably due in part to altimeter sampling issues near the continental boundary. For the three longest tide gauge records, the trends prior to 1993 are 2.2 ± 0.2 , 2.0 ± 0.3 , and 2.0 ± 0.4 mm yr⁻¹ for San Diego (record starts in 1908), San Francisco (1899), and Seattle (1901), respectively, compared to post-1993 trends of -0.3 ± 3.8 , -1.2 ± 4.3 , -1.0 ± 3.5 mm yr⁻¹. While negative trends occur at each station after 1993, they are not more than two standard deviations separated from the long-term, pre-1993 trends. In particular, the recent NEP negative trends appear to be strongly influenced by a decadal high in sea level during the 1990s.

The similarities in NEP sea level fluctuations along the coast suggest the importance of regional wind forcing, which exhibits large decorrelation scales along the North American coast, and poleward propagating coastal-trapped waves (Enfield and Allen 1980; Chelton and Davis 1982). Notable differences among the time series along the North American coast exist as well, for example the high decadal event in the late 1960s-early 1970s is not evident at San Diego. The main conclusion is that the sea-level trend change in the early 1990s evident in the WTP is not distinguishable in the ETP or NEP due to the presence of decadal variability. In contrast to the WTP, averaging the ETP and NEP time series does not reduce the decadal variations given the high level of covariability at these time scales in the eastern Pacific.

5. Wind forcing, climate modes, and sea level change

During 1990 to 2009, mean ORA-S3 surface wind stress patterns over the Pacific (Fig. 8a) tended to intensify (Fig. 8b). Regions where wind stress trends increase include the northeast and southeast trade winds over the tropics, and the westerlies at mid-latitudes in the NEP. Wind stress trends over other areas of the oceans were weaker than in the Pacific, with the exception of increased northeasterly winds in the North Atlantic. During 1959 to 1989, wind stress trends were weak in the tropical Pacific (Fig. 8c) compared to 1990 to 2009 (Fig. 8b).

The average zonal wind stress across the tropical Pacific (20°S to 20°N latitude, and 150°E to the eastern boundary) shows a steady increase in the strength of the trades from the early 1990s onward (Fig. 9). Prior to 1990 the trade wind amplitude did not vary appreciably over time. The change is appreciable, amounting to a nearly 20% increase in the amplitude of the trades from 1990 to 2009. This temporal change in trade wind stress matches the sea level increase observed in the WTP. Near the equator, increasing wind stress contributes to higher WTP sea level due to a balance between wind stress and zonal pressure gradients. Off the equator, the strengthening of the Pacific trades leads to a negative trend in wind stress curl and an increase in downward Ekman pumping, $w_e = \nabla \times \vec{\tau}/(\rho f)$, where $\vec{\tau}$ is the surface wind stress, f is the Coriolis parameter, and ρ is the density of air (Fig. 10). As demonstrated by Qiu and Chen (2010), the w_e tendency favors increasing water levels over the central and western part of the basin due to local wind-driven convergences and westward Rossby wave propagation of positive sea level anomalies. The observed extrema in the WTP sea-level trend during 1993 to 2009 occur off the equator near 10°S and 10°N

(Fig. 3), which highlights the importance of the wind stress curl forcing in those latitude bands.

The correspondence of sea level with the PDO and NPGO, two dominant climate modes in the North Pacific, next is examined. The PDO is the first principal component of North Pacific SST variability in the region poleward of 20°N (Mantua et al. 1996); the NPGO is the second principal component of model-derived SSH (similar results follow from using model SST) in the region bounded by 180°W to 110°W, 25°N to 62°N (Di Lorenzo et al. 2008). The average of the tide gauge records at Seattle, San Francisco, and San Diego, with a linear trend removed, is used to represent NEP sea level variations along the coast of North America (Fig. 11a). The NEP sea level correlation with the NPGO is high (and negative, $r = -0.63$, $p < 0.05$, p values for the correlations r are based on a Monte Carlo analysis of red-noise synthetic data) compared to the correlation with the PDO ($r = 0.32$, $p > 0.05$). Likewise, the WTP sea level correlation with the NPGO is high (and positive, $r = 0.58$, $p < 0.05$) compared to the correlation with the PDO ($r = 0.11$, $p > 0.05$). Visually, the NEP sea level and the NPGO index exhibit similar decadal fluctuations, although the amplitude of the peak sea level during the 1980s is larger than the NPGO compared to other high events (Fig. 11a). WTP sea level and the NPGO co-vary to a degree prior to 1990, but the correspondence breaks down later in the record when WTP sea level continues to rise and the NPGO does not (Fig. 11b).

The global wind stress patterns associated with the PDO and NPGO are assessed by regressing wind stress on the two indices in a multiple regression. Similar to the findings of Di Lorenzo et al. (2008), the PDO corresponds to wind field perturbations in the Aleutian Low region (Fig. 12a), whereas the NPGO describes counter-rotating winds at mid and high

latitudes in the NEP, as well as patterns with a broader global extent than the PDO (Fig. 12b). The NPGO wind pattern resembles the mean wind stress field (Fig. 8a), suggesting that the NPGO in part captures the spin-up and spin-down of the mean atmospheric circulation over the Pacific. The poor correspondence between observed sea levels and the PDO suggests that the primary wind anomalies associated with the PDO at decadal and interdecadal time scales are too far north to impact sea levels in the WTP and NEP regions.

The positive phase of the NPGO corresponds to increased easterly trade winds, mid-latitude westerlies, and northerly winds in the NEP south of 40°N . These wind patterns contribute to a positive sea level anomaly response in the WTP, and negative in the ETP and NEP via local forcing and longwave propagation, which matches the positive and negative correlations between the NPGO index and NEP and WTP sea levels, respectively. North of 40°N , the PDO tends to dominate the local wind forcing and further research is needed to understand wind-driven sea level variations at Ketchikan and farther north along the Alaskan coast. The NEP and WTP sea level co-variations with the NPGO are similar to the SSH response noted by Di Lorenzo et al. (2008). The correlations of decadal fluctuations in NEP and WTP sea level with the NPGO suggest a sea level response to modulations in the mean wind field; however, the WTP sea-level trend since the 1990s appears to be associated with a shift to increasing trade winds that is not captured by the NPGO index, presumably because the NPGO is based on model SSH fields north of 25°N and the trade wind amplification occurs south of this region.

6. Recent warming trends

Other notable indications of a trend shift in tropical atmospheric circulation since the early 1990s have occurred. Chen et al. (2002) analyzed satellite observations to show that the tropics emitted more long-wave radiation and reflected less short-wave radiation from 1985-2000, with most of the change occurring after 1990. Similar trends in upper tropospheric humidity, cloud cover, surface air temperature, and atmospheric vertical velocity led Chen et al. (2002) to conclude that there has been a strengthening of the Hadley and Walker circulations since the early 1990s. To illustrate this point, a principal component analysis (PCA) of five-year mean OLR is computed using the NOAA Interpolated OLR global dataset (Liebmann and Smith 1996). The first PCA mode, which explains 43.7% of the OLR variability, has a spatial pattern that is positive over most of the northern hemisphere and negative in the tropical convergence zones of the Indo-Pacific region (Fig. 13a). The time dependence of mode 1 exhibits a positive trend that increases after 1990 (Fig. 13b). Thus, mode 1 describes broad positive OLR trends that couple with negative trends in the tropical convergence zones, which are indicative of increased tropical convection and intensified trade winds, consistent with the results of section 5. A similar OLR decadal mode was reported by Allan and Slingo (2002).

Changes in SST since the mid-1980s are investigated using the NOAA OI-SST dataset. The dominant PCA mode, which explains 50.5% of the five-year averaged SST variability, is positive in amplitude over much of the tropics and northern hemisphere (Fig. 14a). The mode 1 amplitude is negative in the ETP and the NEP since the early 1990s, in regions where the winds have intensified over that period (Fig. 8b). The time dependence of

mode 1 exhibits a positive trend, such that SST increases over much of the world oceans, and decreases in the regions of enhanced winds in the Pacific, presumably due in part to increased wind-driven mixing and evaporation. The pattern appears to be a combination of the two leading PCA modes computed by Compo and Sardeshmukh (2010) based on the Hadley Centre Sea Ice and Sea Surface Temperature data (HadISST) (1871-2006). The OI-SST time series is too short to evaluate a SST trend change in the early 1990s.

To explore multi-decadal time variability of SST in more detail, the ICOADS dataset is used to extend SST back to the mid-twentieth century. The ICOADS dataset is used instead of HadISST or other extended reconstructions to avoid ambiguities in SST interpolation for earlier time periods when data were sparse. The mode 1 spatial pattern from the OI-SST analysis is regressed on the ICOADS data producing an extended time series of mode 1 amplitude. The time dependence is similar to the OI-SST mode 1 during the period when the two datasets overlap (Fig. 14b). The longer ICOADS time series includes a trend shift in the early 1990s. Thus, SST, OLR, surface wind stress, and WTP sea level all exhibit similar trend increases in the 1990s (Fig. 15), although SST tends to flatten out at the end of the record compared to the other variables.

7. Summary and Discussion

Since the early 1990s, an intensification of the trade winds over the tropical Pacific is linked to the global hot spot of sea-level rise in the WTP. The rising sea levels are a dynamical response to wind-stress forcing, or a redistribution of water. The observed sea-level trends feature two maxima on either side of the equator, emphasizing the importance

of off-equatorial wind stress curl. Weak negative sea-level trends in the NEP over the same time period are indistinguishable from decadal sea-level oscillations, which overwhelm short-term trend estimates unless the ratio of trend signal to decadal noise is large, as is the case in the WTP.

A WTP sea level change in the 1990s also has been noted and related to enhanced trade wind forcing by Feng et al. (2010) and Carton et al. (2005). Feng et al. (2010) was concerned primarily with the variability of shallow overturning circulation in the Pacific and used sea level differences as a proxy for these changes. They limited their analysis to the tide gauge record at Pohnpei in the WTP, and noted that stations like Guam exhibited unusual drifts. In this study, which uses more and longer tide gauge records than Feng et al. (2010), the unusual drifts are found to characterize a regional trend shift in sea level. Moreover, it is demonstrated that a shift of this magnitude has only occurred once in the regionally averaged trends since the mid-twentieth century. Carton et al. (2005) examined the 1993-2001 period, which is too short of a record to appreciate the duration and magnitude of the trade wind intensification. A similar type of long-term, wind-forced shift in regional sea-levels has been reported by Han et al. (2010) in the Indian Ocean. The changes in the Indian Ocean are considerably weaker, ranging between $\pm 2\text{mm yr}^{-1}$, and occur over a longer time span, 1961 to 2008, than the Pacific trend shift considered in this study.

The WTP sea-level trend may be part of a multi-decadal to centennial fluctuation in sea level as opposed to a secular change; however, this is difficult to assess as tide gauge and other in situ measurements in the tropics generally do not date back prior to the late 1940s. One piece of evidence that does suggest a long-term fluctuation is that the sea-level trends at Guam and Kwajalein for the period from about 1950 to 1993 are lower than the 1.7

mm yr⁻¹ global mean sea-level trend reported for the second half of the twentieth century (Bindoff et al. 2007). The low sea-level trends may be symptomatic of a prolonged period of weaker than normal trade winds. The sea level reconstructions of Church et al. (2006) show a 1950 to 2001 trend pattern in the WEP similar to the 1993-2009 pattern but significantly weaker and with opposite sign, which suggests a weakening trade wind tendency for that period. Such a trend, however, does not appear in the ORA-S3 winds (Fig. 8c, Fig. 9). The WTP sea level trend increase bears some resemblance to other measures of global climate state, such as globally-averaged surface air temperature (Hansen et al. 2010), although the shift in air temperatures occurs a decade or so earlier than the WTP shift. In the mean air temperature time series, 1950-1990 is a period of relatively low trends. Analyses of in situ datasets and other reanalysis wind products are needed to explore these issues further.

Decadal sea level fluctuations in the WTP and NEP correlate with the NPGO index, although not the PDO index. Wind patterns associated with the NPGO suggest that decadal modulations of the tropical trades and sub-tropical westerlies drive sea level variability in the WTP and NEP. The NPGO however does not capture the WTP trend increase, suggesting that the post-1990s trade wind enhancement does not strongly project onto SSH patterns north of 25°N, which is where the NPGO index is derived from model simulations.

It is speculated that the Pacific trade wind enhancement since the early 1990s is fueled by an increase in latent heat content in a warming atmosphere, which invigorates deep convection in the tropics and speeds up the atmospheric circulation. This generally supports the notion of a strengthening Hadley circulation in recent decades (Chen et al. 2002; Mitras and Clement 2005). The hypothesis seems to contradict observational and modeling studies that suggest a weakening tropical circulation in the Pacific and an enhanced El Niño-like state

in response to global warming (Vecchi et al. 2006; Zhang and Song 2006; Vecchi and Soden 2007; Yu and Zwiers 2010). Multi-model averages from atmosphere-ocean general circulation models used in the Intergovernmental Panel on Climate Change Fourth Assessment Report (IPCC AR4) tend to indicate a weakening tropical circulation in response to an imposed warming signal (see Collins et al. (2010) for a summary), which has been linked to parameterizations of weak vertical mass exchange rates in the tropics (Held and Soden 2006). A major difference between the present results and these previous studies is one of time scales. Global warming trends generally are estimated over long time periods commensurate with the build-up of greenhouse gases (e.g., since 1860, Vecchi et al. (2006)). Nevertheless, the recent trade wind increase does appear to be linked to warming signals (section 6), in which case the ability of coupled models to capture this sort of variability comes into question (Wielicki et al. 2002).

A number of studies (Church et al. 2004; Holgate and Woodworth 2004; Church and White 2006; Jevrejeva et al. 2006; Holgate 2007; Domingues et al. 2008; Merrifield et al. 2009) have shown that the rate of global sea-level has increased over roughly the same time period as the WTP trend shift reported here. Whether this recent global trend increase is unusual or not over the past century remains an open question. The present results are similar to those of Merrifield et al. (2009) in that both the global and WTP regional trend increases in the early 1990s appear to be large amplitude, unusual occurrences since the mid-twentieth century. Earlier periods are difficult to assess given the diminishing number of tide gauges back in time, particularly before 1950. It appears that the recent change in global sea level is associated with increased rates of ocean warming and ice melt, which have been reported to occur since the early 1990s (see Bindoff et al. (2007) for a review), in

which case the change in regional WTP sea level likely is a wind-forced response linked to the same warming trends. A better understanding of the causes of the trade wind enhancement is needed to understand the relationship between the global and WTP regional trend increases, as well as to predict how water levels in the WTP will change in coming decades, which is critical in terms of sea-level rise impacts given the large number of populated, low-lying atolls and islands in the hot spot region.

Acknowledgments.

Discussions with Eric Firing helped shape the analysis and interpretation of the results. Critical comments by two anonymous reviewers greatly improved the paper. Shikiko Nakahara assisted with the data analysis. The altimeter products were produced by Ssalto/Duacs and distributed by AVISO, with support from the Centre National d'Etudes Spatiales (CNES). Support was provided by the Office of Climate Observations, NOAA (NA17RJ1230), and NASA (1278112).

REFERENCES

- Allan, R. P. and A. Slingo, 2002: Can current climate model forcings explain the spatial and temporal signatures of OLR variations? *Geophys. Res. Lett.*, **29**, No. 7, 10.1029/2001GL014620.
- Balmaseda, M. A., A. Vidard, and D. L. Anderson, 2008: The ECMWF ocean analysis system: ORA-S3. *Monthly Wea. Rev.*, **136**, 3018–3034.
- Bindoff, N. L., et al., 2007: Observations: Oceanic climate change and sea level. *Climate Change 2007: The Physical Science Basis. Contribution of Working Group I to the Fourth Assessment Report of the Intergovernmental Panel on Climate Change*, S. Solomon, D. Qin, J. Manning, Z. Chen, M. Marquis, K. B. Averyt, M. Tignor, and H. L. Miller, Eds., Cambridge University Press, Cambridge, United Kingdom and New York, NY, USA.
- Carton, J. A., B. S. Giese, and S. A. Grodsky, 2005: Sea level rise and the warming of the oceans in the Simple Ocean Data Assimilation (SODA) ocean reanalysis. *J. Geophys. Res.*, **110**, C09006, doi:10.1029/2004JC002817.
- Chelton, D. B. and R. E. Davis, 1982: Monthly mean sea level variability along the west coast of North America. *J. Phys. Oceanogr.*, **12**, 757–784.
- Chen, J. Y., B. E. Carlson, and A. D. Del Genio, 2002: Evidence for strengthening of the tropical general circulation in the 1990s. *Science*, **295**, 838–841.

- Chen, J. Y., A. D. Del Genio, B. E. Carlson, and M. G. Bosilovich, 2008: The spatiotemporal structure of twentieth-century climate variations in observations and reanalyses. Part I: Long-term trend. *J. Climate*, **21**, 2611–2633.
- Church, J. A. and N. J. White, 2006: A 20th century acceleration in global sea level rise. *Geophys. Res. Lett.*, **33**, L01 602, doi:10.1029/2005GL024 826.
- Church, J. A., N. J. White, R. Coleman, K. Lambeck, and J. X. Mitrovica, 2004: Estimates of the regional distribution of sea level rise over the 1950 to 2000 period. *J. Climate*, **17**, 2609–2625.
- Church, J. A., N. J. White, and J. R. Hunter, 2006: Sea-level rise at tropical Pacific and Indian Ocean islands. *Global Planet. Change*, **53**, 155–168.
- Clarke, A. J. and A. Lebedev, 1996: Long-term changes in the equatorial Pacific trade winds. *J. Climate*, **9**, 1020–1029.
- Collins, M., et al., 2010: The impact of global warming on the tropical Pacific Ocean and El Niño. *Nature Geosci.*, **3**, 391–397.
- Compo, G. P. and P. D. Sardeshmukh, 2010: Removing ENSO-related variations from the climate record. *J. Climate*, **23**, 1957–1978.
- Cummins, P. F. and H. J. Freeland, 2007: Variability of the North Pacific Current and its bifurcation. *Prog. Oceanogr.*, **75**, 253–265.
- Di Lorenzo, E., et al., 2008: North Pacific Gyre Oscillation links ocean climate and ecosystem change. *Geophys. Res. Lett.*, **35**, L08 607,doi:10.1029/2007GL032 838.

- Domingues, C. M., J. A. Church, N. J. White, P. J. Gleckler, S. E. Wijffels, P. M. Barker, and J. R. Dunn, 2008: Improved estimates of upper-ocean warming and multi-decadal sea-level rise. *Nature*, **453**, 1090–1093.
- Enfield, D. B. and J. S. Allen, 1980: On the structure and dynamics of monthly mean sea level anomalies along the Pacific coast of North and South America. *J. Phys. Oceanogr.*, **10**, 557–578.
- Feng, M., M. J. McPhaden, and T. Lee, 2010: Decadal variability of the Pacific subtropical cells and their influence on the southeast Indian Ocean. *Geophys. Res. Lett.*, **37**, L09 606, doi:10.1029/2010GL042 796.
- Firing, Y. L., M. A. Merrifield, T. A. Schroeder, and B. Qiu, 2004: Interdecadal sea level fluctuations at Hawaii. *J. Phys. Oceanogr.*, **34**, 2514–2524.
- Fu, L.-L. and B. Qiu, 2002: Low-frequency variability of the North Pacific Ocean: The roles of boundary-and wind-driven baroclinic Rossby waves. *J. Geophys. Res.*, **107**, 3220, doi:10.1029/2001JC001 131.
- Han, W., et al., 2010: Patterns of Indian Ocean sea-level change in a warming climate. *Nat. Geo.*, **3**, 546–550.
- Hansen, J., R. Ruedy, M. Sato, and K. Lo, 2010: Global surface temperature change. *Rev. Geophys.*, **48**, RG4004, doi:10.1029/2010RG00 345.
- Held, I. M. and B. J. Soden, 2006: Robust responses of the hydrological cycle to global warming. *J. Climate*, **19**, 5686–5699.

- Holgate, S. J., 2007: On the decadal rates of sea level change during the twentieth century. *Geophys. Res. Lett.*, **34**, L01 601, doi:10.1029/2006GL028 492.
- Holgate, S. J. and P. L. Woodworth, 2004: Evidence for enhanced coastal sea level rise during the 1990s. *Geophys. Res. Lett.*, **31**, L07 305, doi:10.1029/2004GL019 626.
- Jevrejeva, S., A. Grinsted, J. C. Moore, and S. Holgate, 2006: Nonlinear trends and multiyear cycles in sea level records. *J. Geophys. Res.*, **111**, C09 012, doi:10.1029/2005JC003 229.
- Köhl, A., D. Stammer, and B. Cornuelle, 2007: Interannual to decadal changes in the ECCO Global Synthesis. *J. Phys. Oceanogr.*, **37**, 313–337.
- Lageroef, G. S. E., 1997: Interdecadal variations in the Alaska Gyre. *J. Phys. Oceanogr.*, **25**, 2242–2258.
- Lee, T. and M. J. McPhaden, 2008: Decadal phase change in large-scale sea level and winds in the Indo-Pacific region at the end of the 20th century. *Geophys. Res. Lett.*, **35**, L01 605, doi:10.1029/2007GL032 419.
- Li, B. and A. J. Clarke, 1994: An examination of some ENSO mechanisms using interannual sea level at the eastern and western boundaries and the zonally averaged equatorial wind. *J. Phys. Oceanogr.*, **24**, 681–690.
- Liebmann, B. and C. A. Smith, 1996: Description of a complete (interpolated) outgoing longwave radiation dataset. *Bull. Am. Met. Soc.*, **77**, 1275–1277.
- Lombard, A., G. Garric, and T. Penduff, 2009: Regional patterns of observed sea level change: insights from a $1/4^\circ$ global ocean/sea-ice hindcast. *Ocean Dyn.*, **59**, 433–449.

- Mantua, N. J., S. R. Hare, Y. Zhang, J. M. Wallace, and R. C. Francis, 1996: A Pacific interdecadal climate oscillation with impacts on salmon production. *Bull. Am. Met. Soc.*, **77**, 1275–1277.
- McPhaden, M. J. and D. Zhang, 2002: Slowdown of the meridional overturning circulation in the upper Pacific Ocean. *Nature*, **415**, 603–608.
- McPhaden, M. J. and D. Zhang, 2004: Pacific Ocean circulation rebounds. *Geophys. Res. Lett.*, **31**, L18 301, doi:10.1029/2004GL020 727.
- Merrifield, M. A., S. T. Merrifield, and G. T. Mitchum, 2009: An anomalous recent acceleration of global sea level rise. *J. Clim.*, **22**, 5772–5781.
- Mitas, C. M. and A. Clement, 2005: Has the Hadley cell been strengthening in recent decades? *Geophys. Res. Lett.*, **32**, L03 098, doi:10.1029/2004GL021 765.
- Qiu, B. and S. Chen, 2010: Interannual-to-decadal variability in the bifurcation of the North Equatorial Current off the Philippines. *J. Phys. Oceanogr.*, **40**, 2525–2538.
- Timmermann, A., S. McGregor, and F.-F. Jin, 2010: Wind effects on past and future regional sea-level trends in the southern Indo-Pacific. *J. Climate*, **23**, 4429–4437.
- Vecchi, G. A. and B. J. Soden, 2007: Global warming and the weakening of the tropical circulation. *J. Climate*, **20**, 4316–4340.
- Vecchi, G. A., B. J. Soden, A. T. Wittenberg, I. M. Held, A. Leetmaa, and M. J. Harrison, 2006: Weakening of tropical Pacific atmospheric circulation due to anthropogenic forcing. *Nature*, **441**, 73–76.

- Wielicki, B. A., et al., 2002: Evidence for large decadal variability in the tropical mean radiative energy budget. *Science*, **295**, 841–844.
- Woodworth, P. and R. Player, 2003: The Permanent Service for Mean Sea Level: An update to the 21st century. *J. Coastal Res.*, **19**, 287–295.
- Yu, B. and F. W. Zwiers, 2010: Changes in equatorial atmospheric zonal circulations in recent decades. *Geophys. Res. Lett.*, **37**, L05701, doi:10.1029/2009GL042071.
- Zhang, M. and H. Song, 2006: Evidence of deceleration of atmospheric vertical overturning circulation over the tropical Pacific. *Geophys. Res. Lett.*, **33**, L12701, doi:10.1029/2006GL025942.

List of Figures

- 1 The linear trend in satellite altimetry sea surface height (SSH) for the period 1993-2009, based on the Aviso multi-mission altimeter data product . 28
- 2 SSH trends obtained in a multiple regression including the NINO3 index (N) and its Hilbert transform (\tilde{N}). 29
- 3 Map of SSH trends for 1993 to 2009 with the locations of tide gauge stations. 30
- 4 Five-year mean sea level from the Guam and Kwajalein tide gauges. The data are presented relative to the mean of each record computed through 1992. 31
- 5 Five-year mean sea level from tide gauges in the WTP (thick curves) and from the Aviso SSH gridded data nearest the tide gauge station (thin curves). 32
- 6 The spatially averaged sea level in the WTP computed from the tide gauge records in Fig. 5. The solid curve is the average of all records. Prior to the mid-1970s only Guam, Kwajalein, and Pago Pago contribute to the mean. The dashed curve is the average of all the records except Guam, Kwajalein, and Pago Pago. 33
- 7 Five-year mean sea level from tide gauges (thick curves) in the ETP (Santa Cruz) and the NEP, and from the Aviso SSH gridded data nearest the tide gauge stations (thin curves). 34
- 8 Linear trend in ECMWF ORA-S3 wind stress for (a) 1959 to 1989 and (b) 1990 to 2009. 35

9	Comparison of average WTP sea level and the amplitude of zonal wind stress averaged across the Pacific between 20°S to 20°N latitude, and 150°E to the eastern boundary.	36
10	Linear trends in ECMWF ORA-S3 wind stress (vectors) and Ekman pumping velocity (color map) for 1990 to 2009.	37
11	(a) Five-year mean time series of NEP sea level (average of Seattle, San Francisco, and San Diego) compared with the PDO index and -1xNPGO index. Index amplitudes are indicated on the right-hand axis. (b) Five-year mean time series of average WTP sea level compared with the PDO index and NPGO index.	38
12	Five-year mean ECMWF ORA-S3 wind stress regressed on (a) the PDO index, and (b) the NPGO index.	39
13	Spatial (a) and temporal (b) patterns of the first principal component of five-year mean outgoing longwave radiation (OLR).	40
14	Spatial (a) and temporal (b) patterns of the first principal component of five-year mean Optimum Interpolation Sea Surface Temperature (OISST). ICOADS SST is regressed on the mode 1 pattern (a), producing the time series in (b).	41
15	Time series of WTP sea level, mode 1 OLR, mode 1 SST, and average zonal wind stress in the tropical Pacific all show a noticeable increase during the early 1990s. An offset and scale factor have been applied to OLR mode 1, SST mode 1, and mean zonal wind stress to match mean WTP sea level.	42

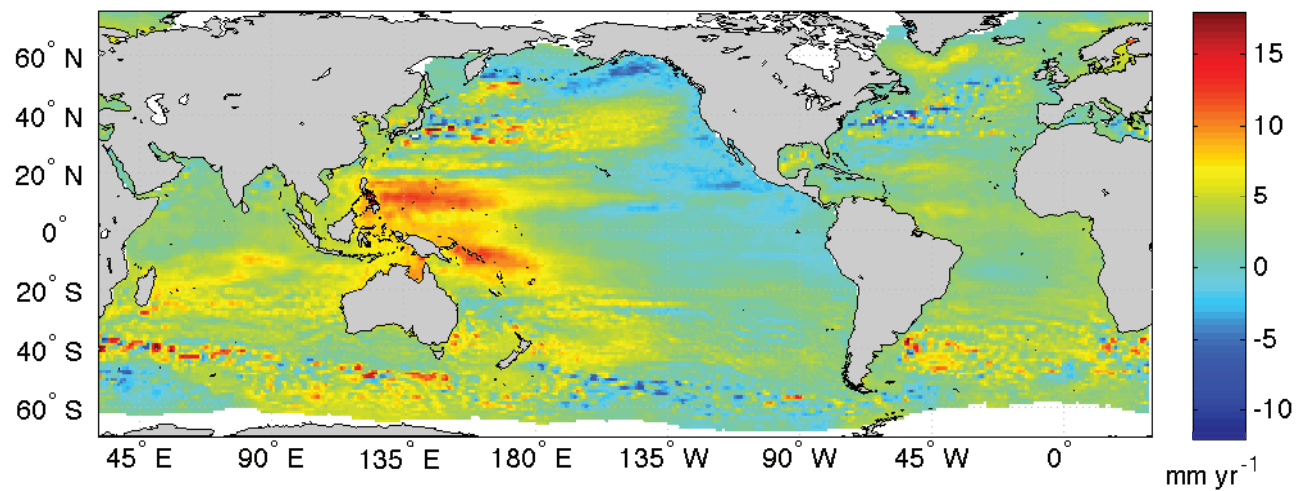


FIG. 1. The linear trend in satellite altimetry sea surface height (SSH) for the period 1993-2009, based on the Aviso multi-mission altimeter data product .

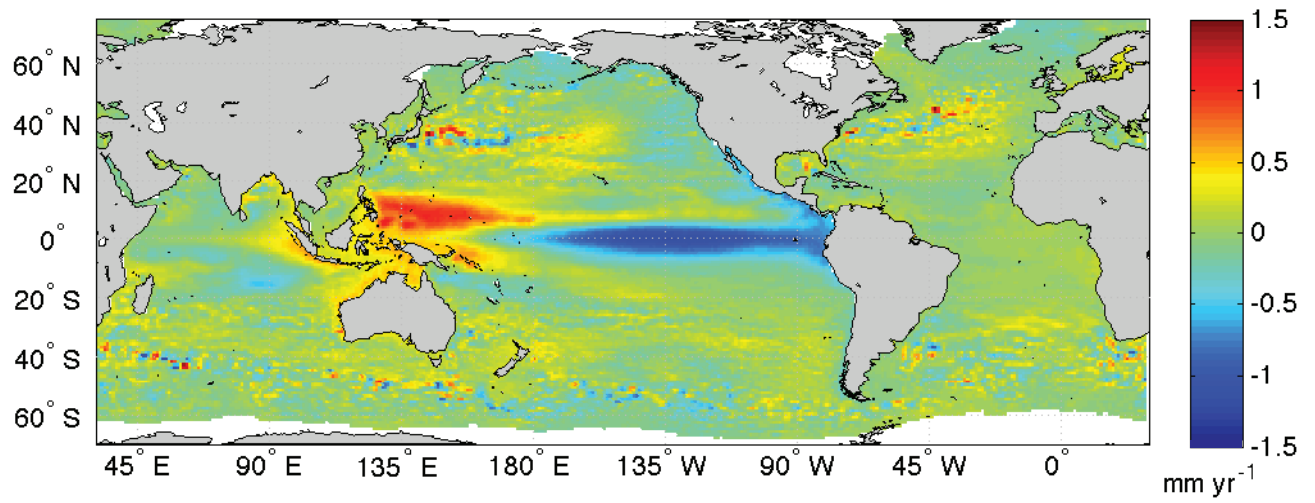


FIG. 2. SSH trends obtained in a multiple regression including the NINO3 index (N) and its Hilbert transform (\tilde{N}).

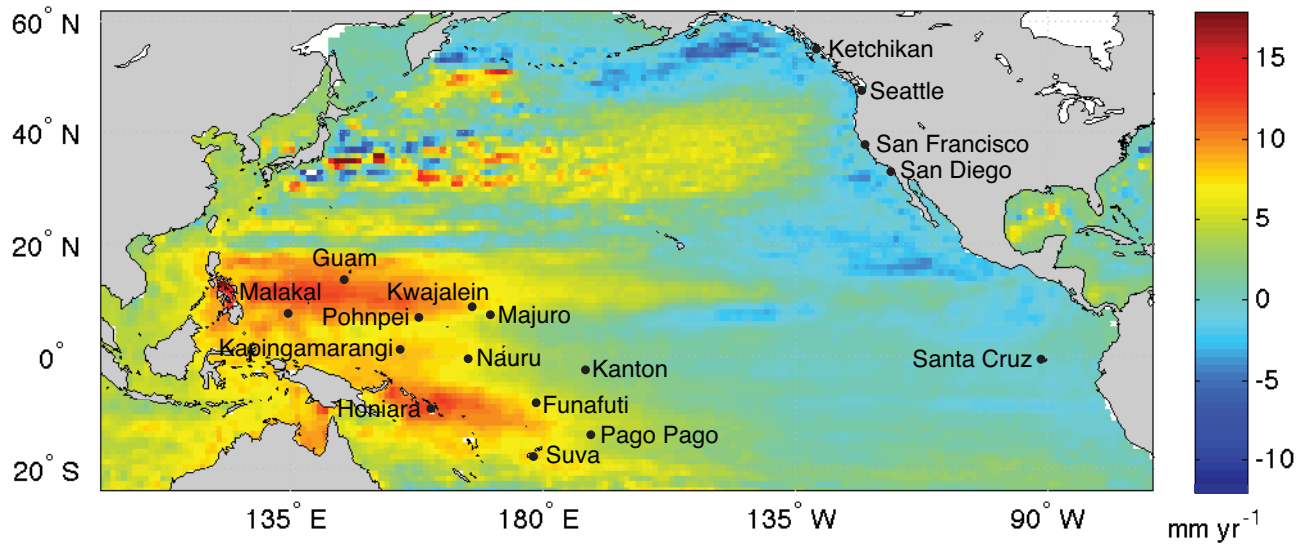


FIG. 3. Map of SSH trends for 1993 to 2009 with the locations of tide gauge stations.

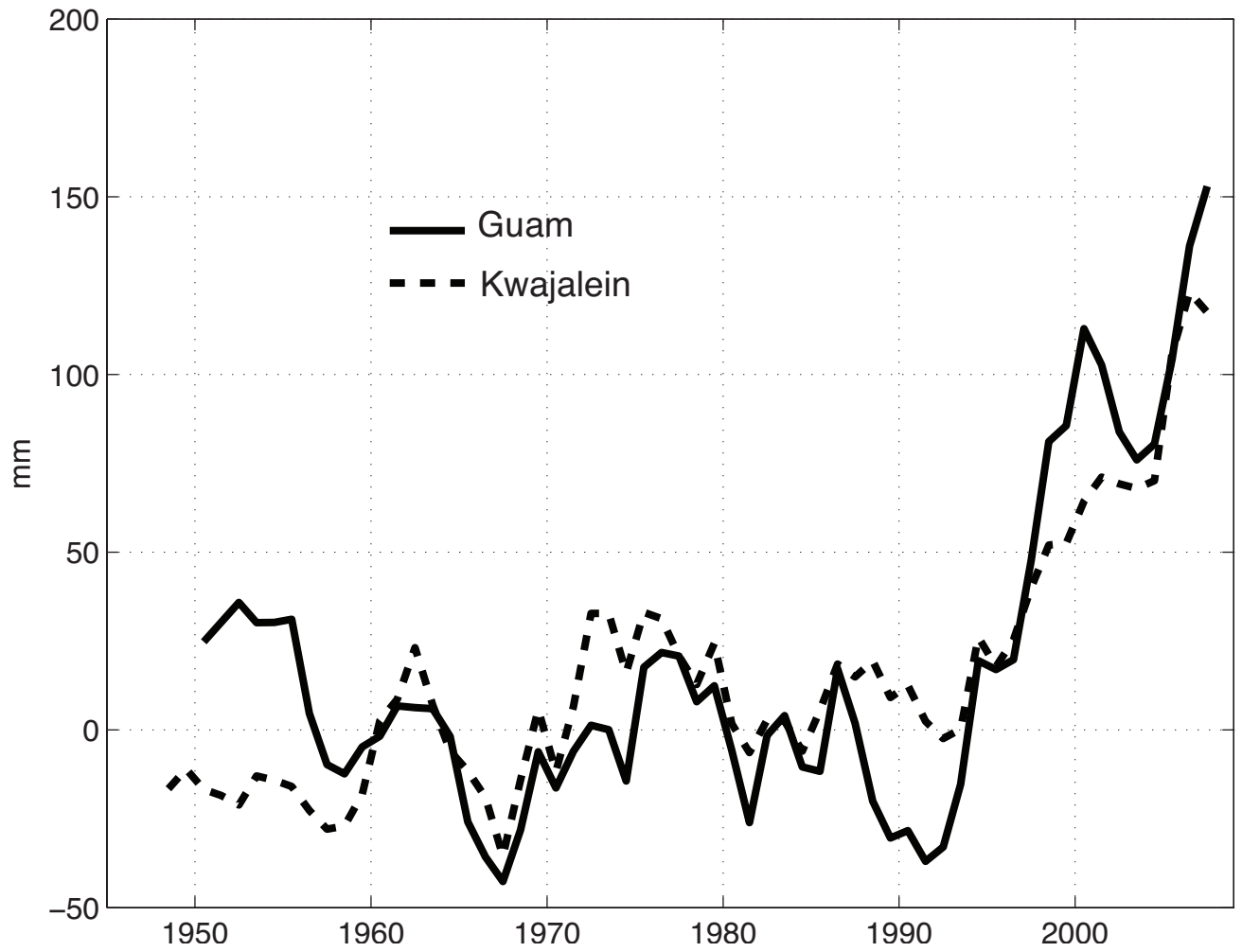


FIG. 4. Five-year mean sea level from the Guam and Kwajalein tide gauges. The data are presented relative to the mean of each record computed through 1992.

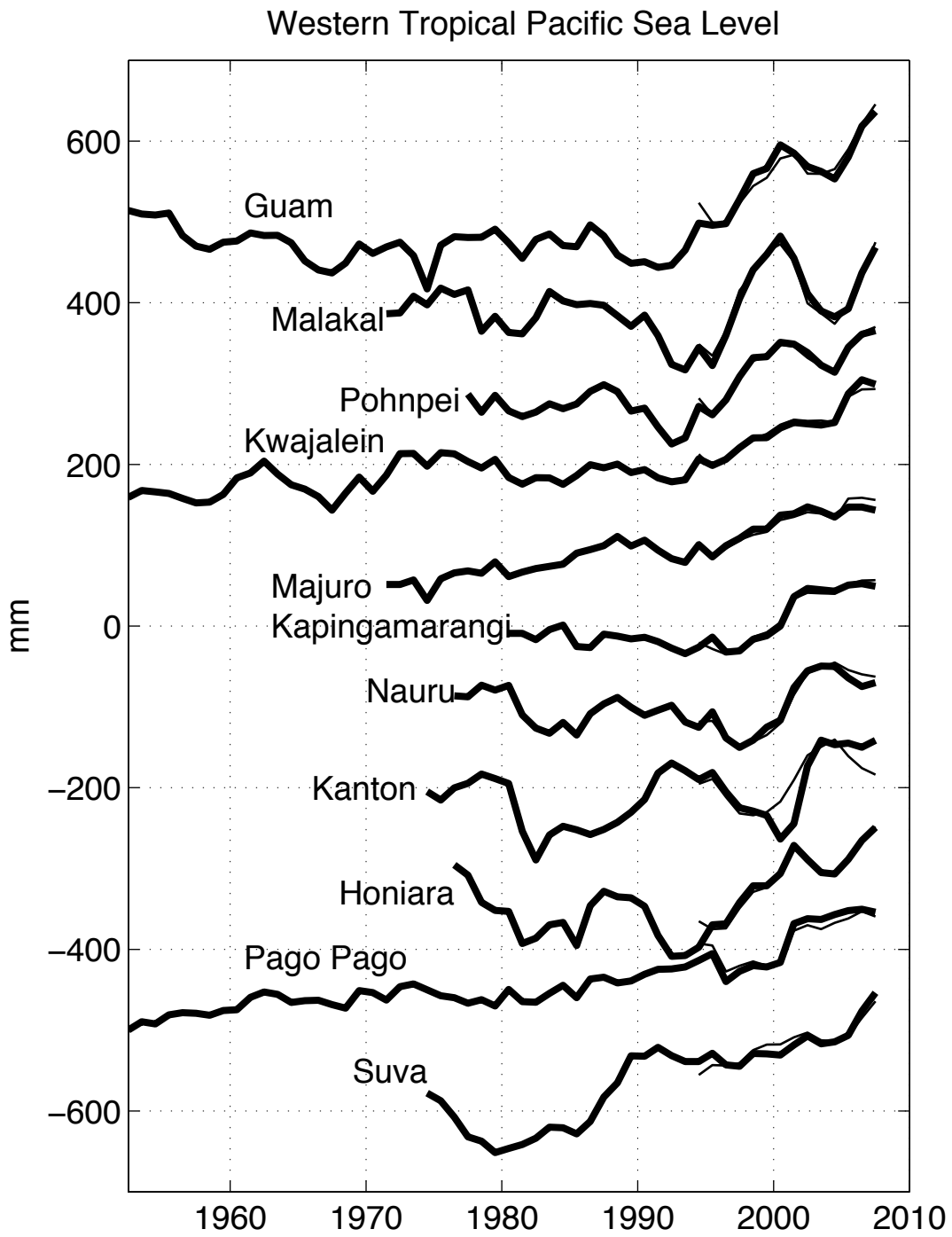


FIG. 5. Five-year mean sea level from tide gauges in the WTP (thick curves) and from the Aviso SSH gridded data nearest the tide gauge station (thin curves).

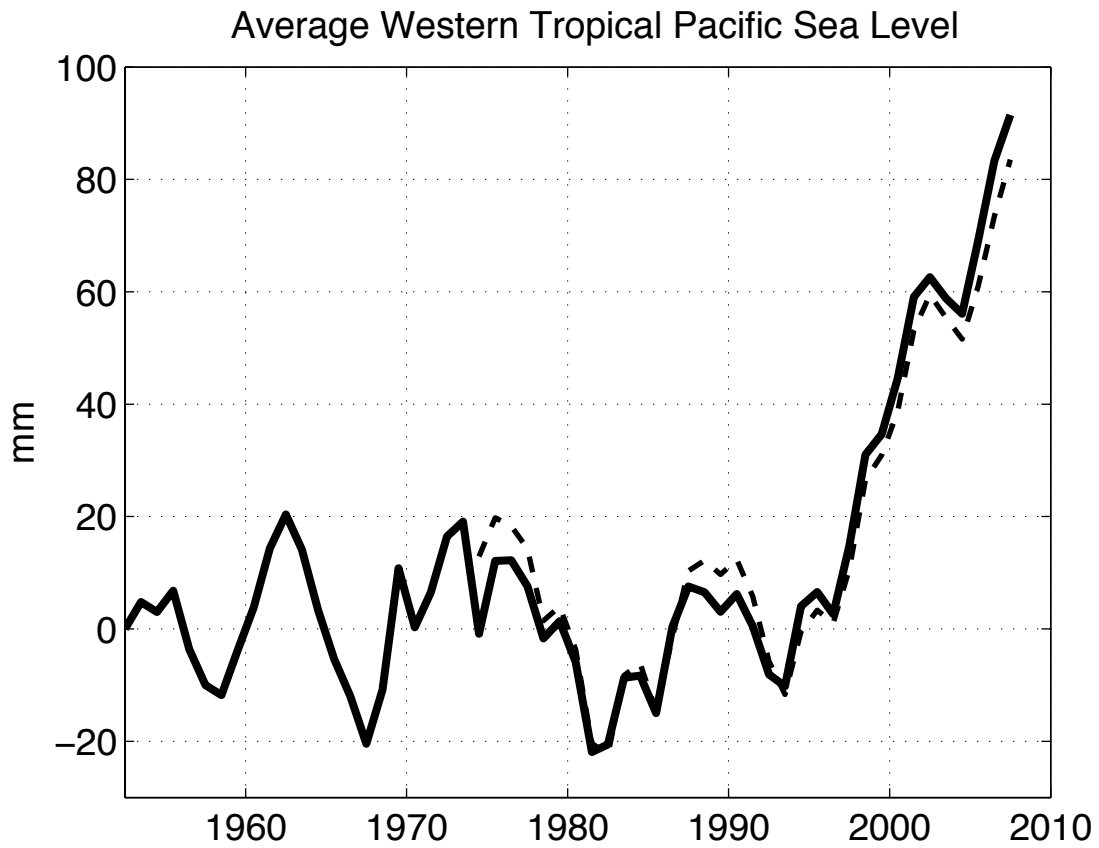


FIG. 6. The spatially averaged sea level in the WTP computed from the tide gauge records in Fig. 5. The solid curve is the average of all records. Prior to the mid-1970s only Guam, Kwajalein, and Pago Pago contribute to the mean. The dashed curve is the average of all the records except Guam, Kwajalein, and Pago Pago.

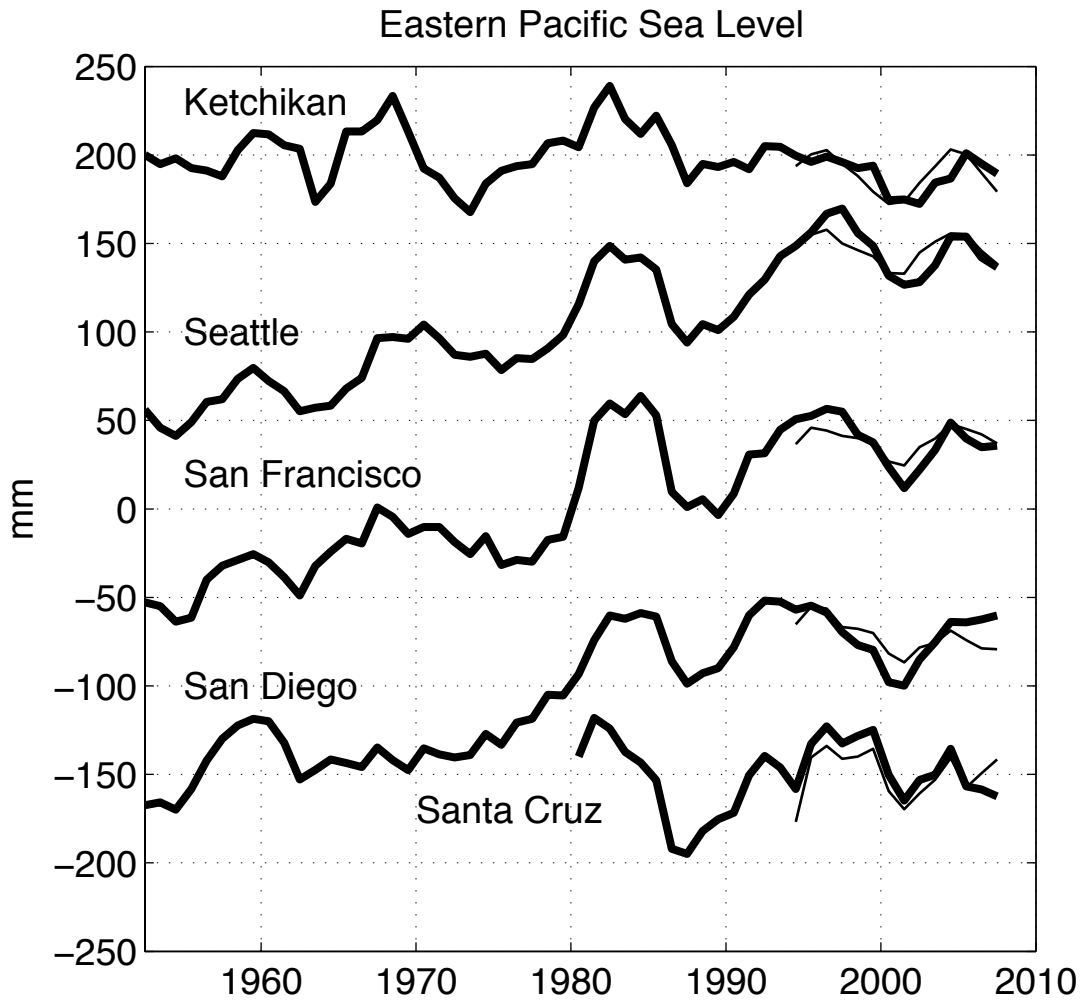


FIG. 7. Five-year mean sea level from tide gauges (thick curves) in the ETP (Santa Cruz) and the NEP, and from the Aviso SSH gridded data nearest the tide gauge stations (thin curves).

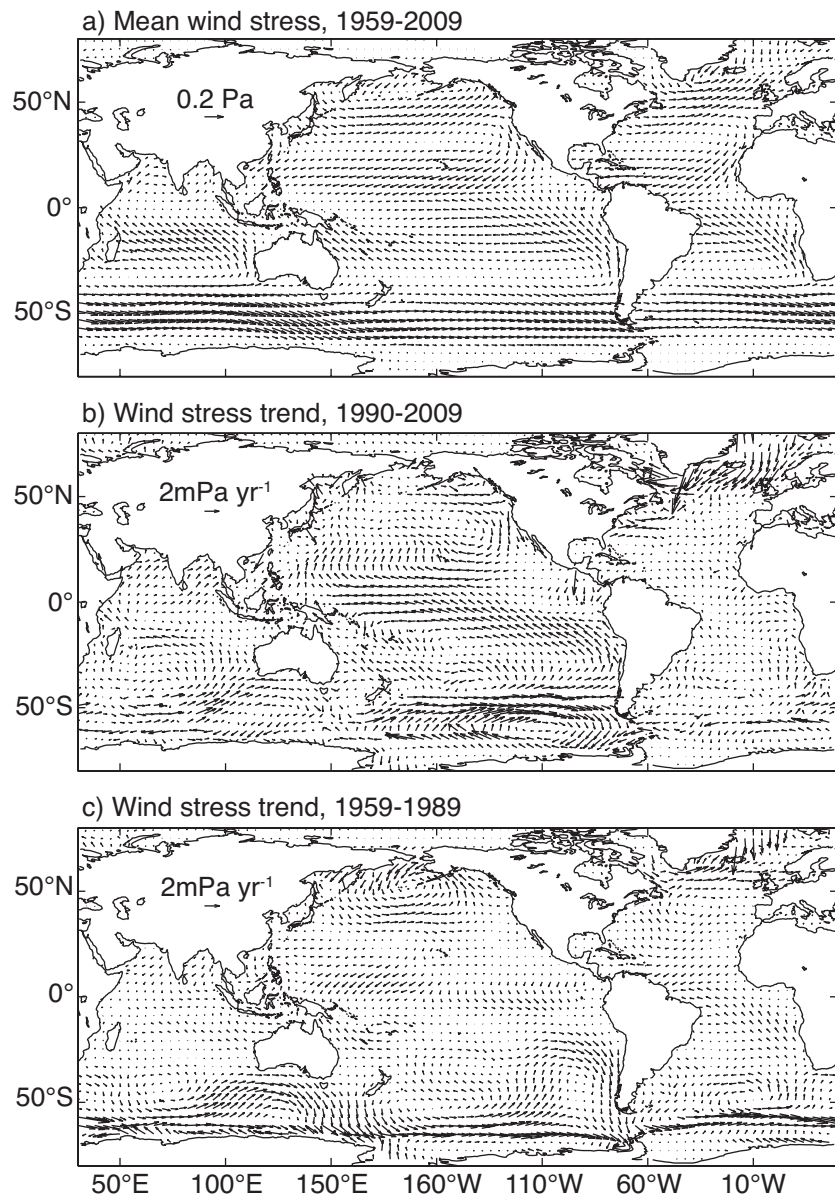


FIG. 8. Linear trend in ECMWF ORA-S3 wind stress for (a) 1959 to 1989 and (b) 1990 to 2009.

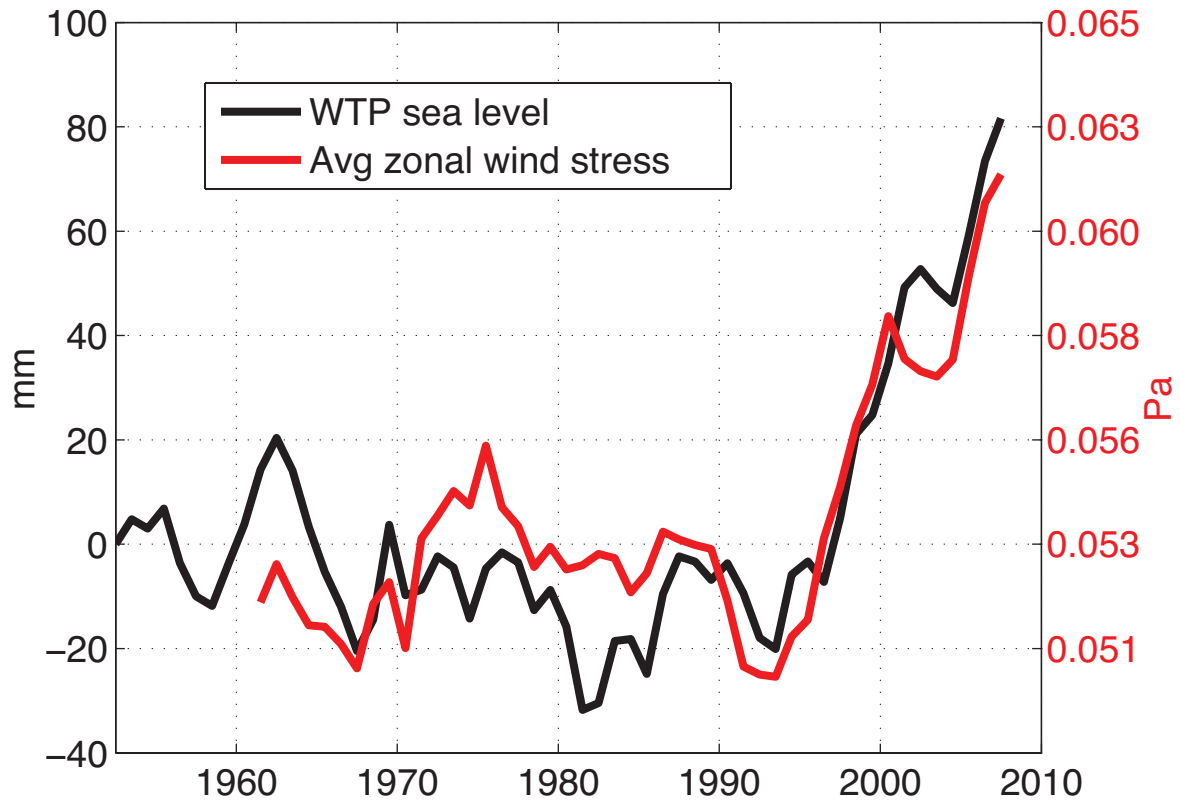


FIG. 9. Comparison of average WTP sea level and the amplitude of zonal wind stress averaged across the Pacific between 20°S to 20°N latitude, and 150°E to the eastern boundary.

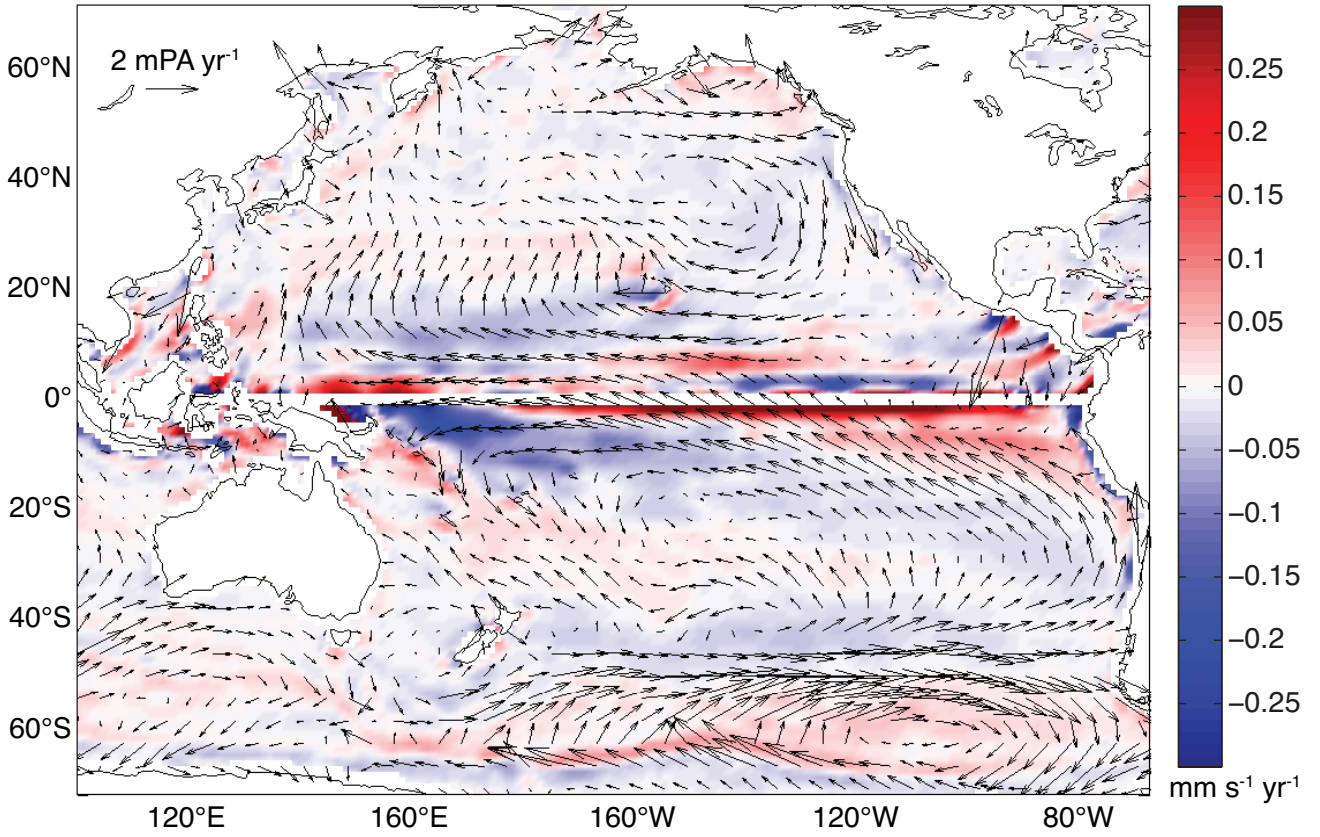


FIG. 10. Linear trends in ECMWF ORA-S3 wind stress (vectors) and Ekman pumping velocity (color map) for 1990 to 2009.

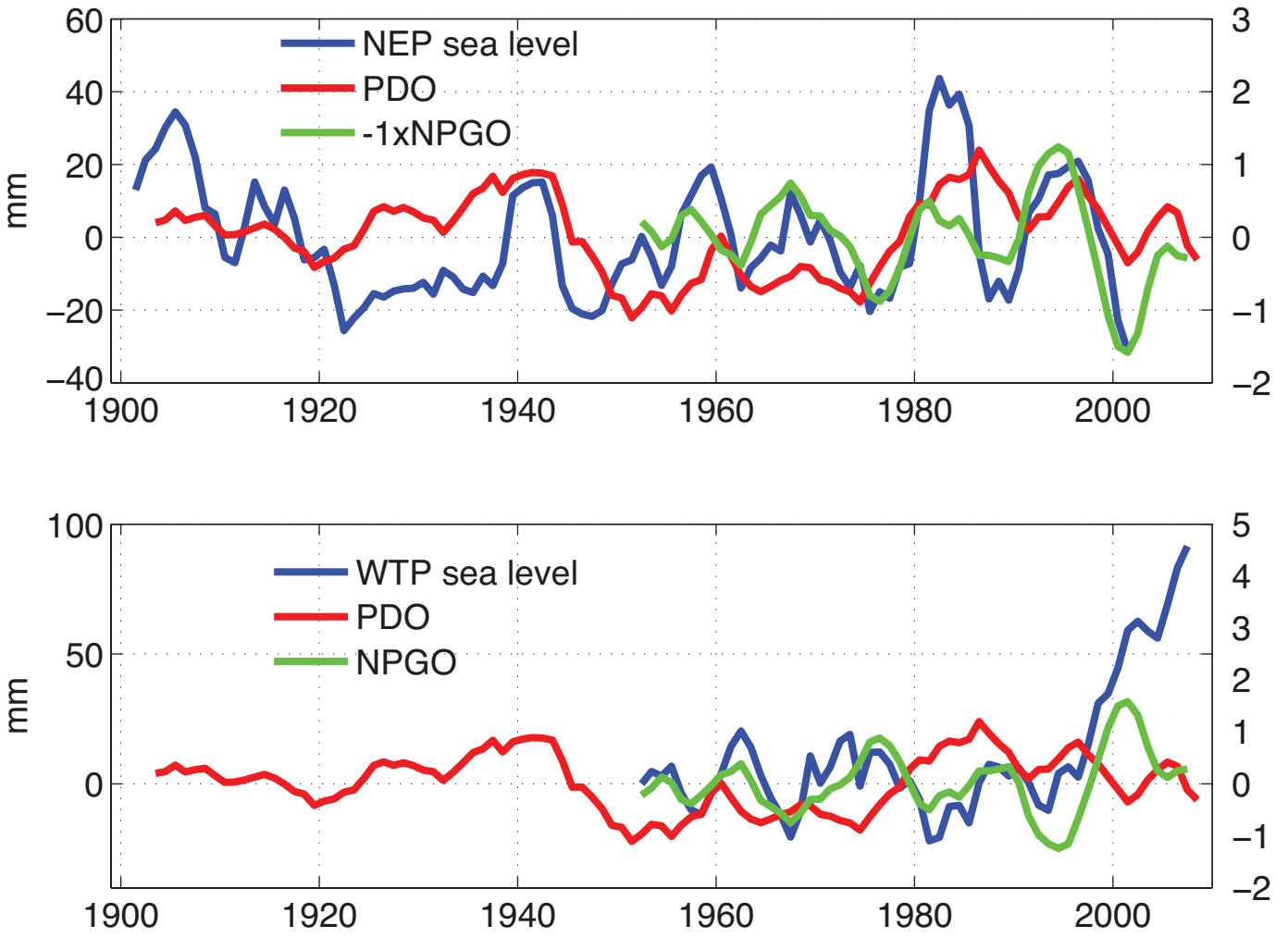


FIG. 11. (a) Five-year mean time series of NEP sea level (average of Seattle, San Francisco, and San Diego) compared with the PDO index and $-1 \times \text{NPGO}$ index. Index amplitudes are indicated on the right-hand axis. (b) Five-year mean time series of average WTP sea level compared with the PDO index and NPGO index.

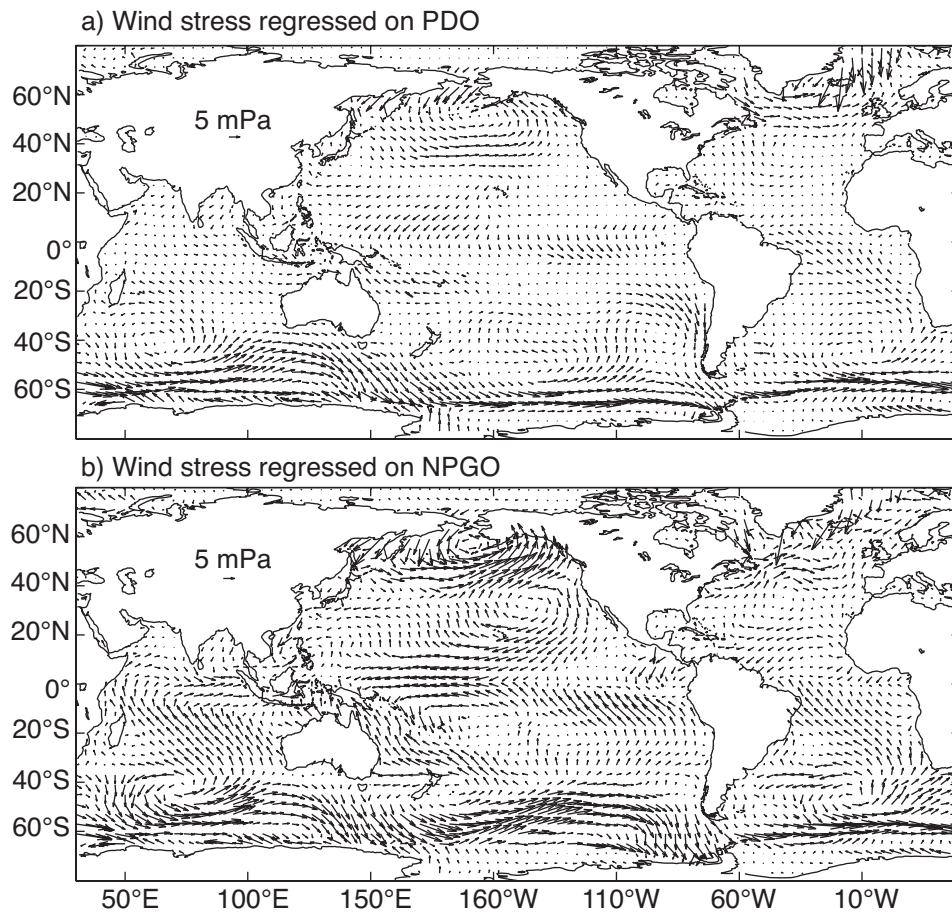


FIG. 12. Five-year mean ECMWF ORA-S3 wind stress regressed on (a) the PDO index, and (b) the NPGO index.

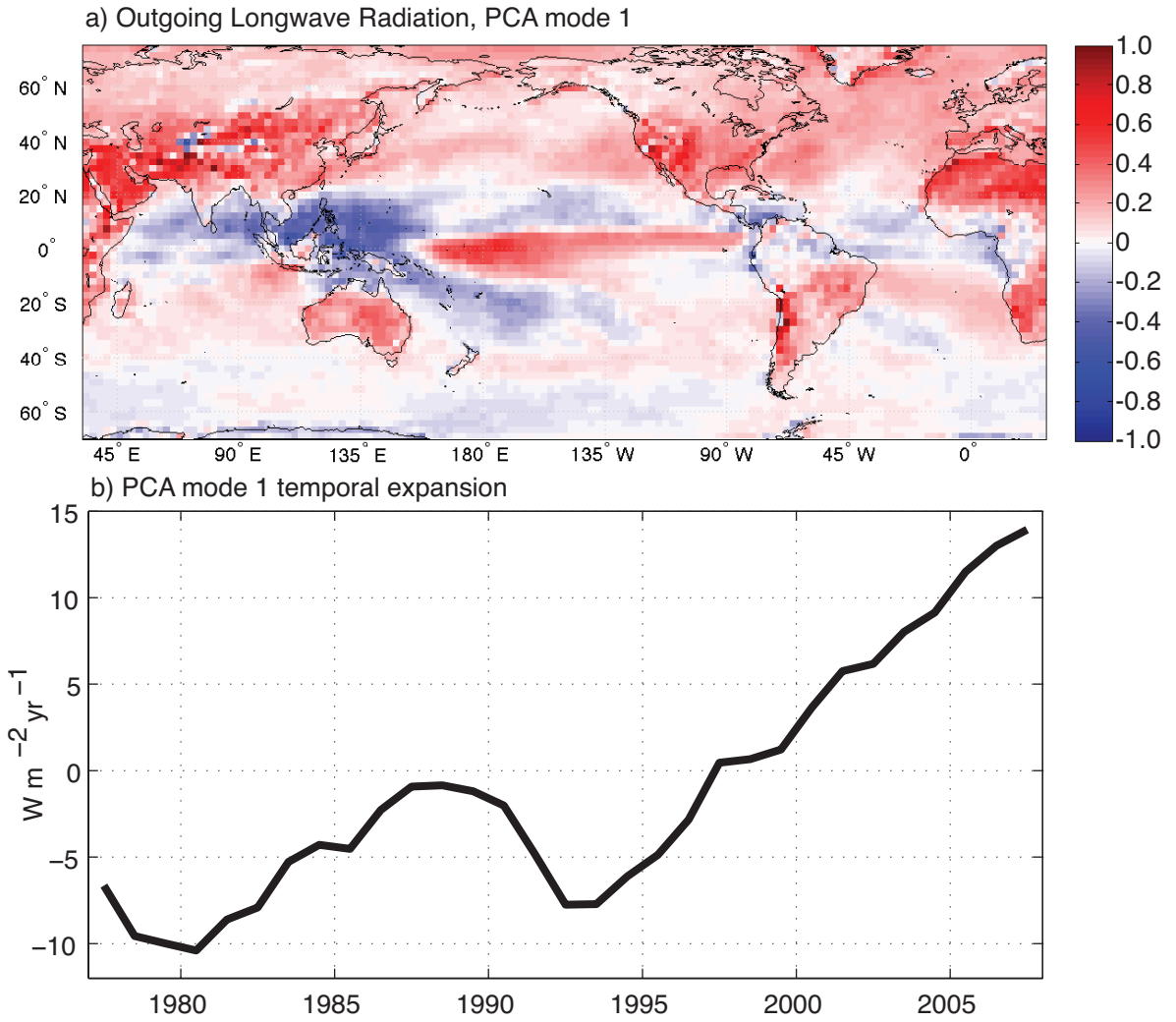


FIG. 13. Spatial (a) and temporal (b) patterns of the first principal component of five-year mean outgoing longwave radiation (OLR).

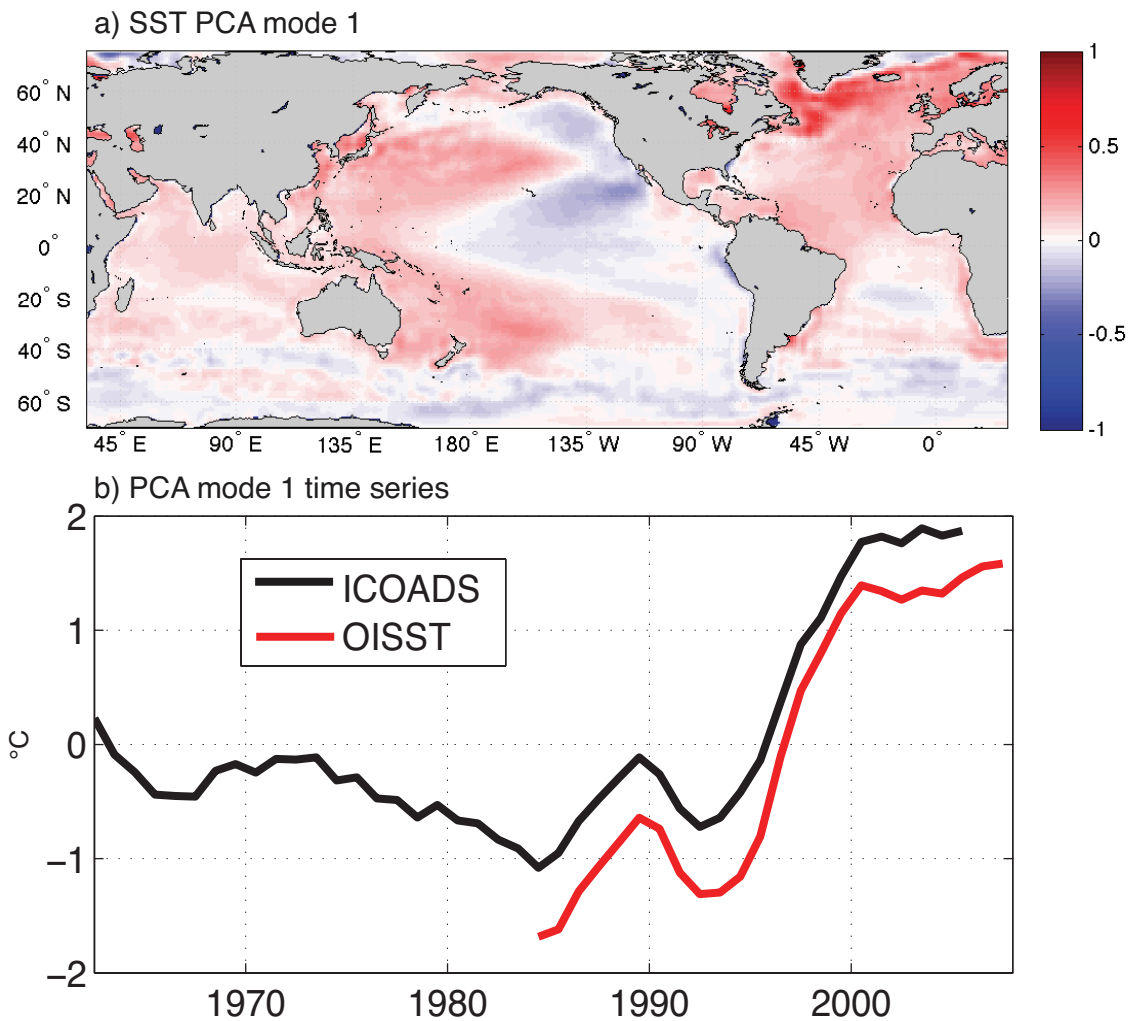


FIG. 14. Spatial (a) and temporal (b) patterns of the first principal component of five-year mean Optimum Interpolation Sea Surface Temperature (OISST). ICOADS SST is regressed on the mode 1 pattern (a), producing the time series in (b).

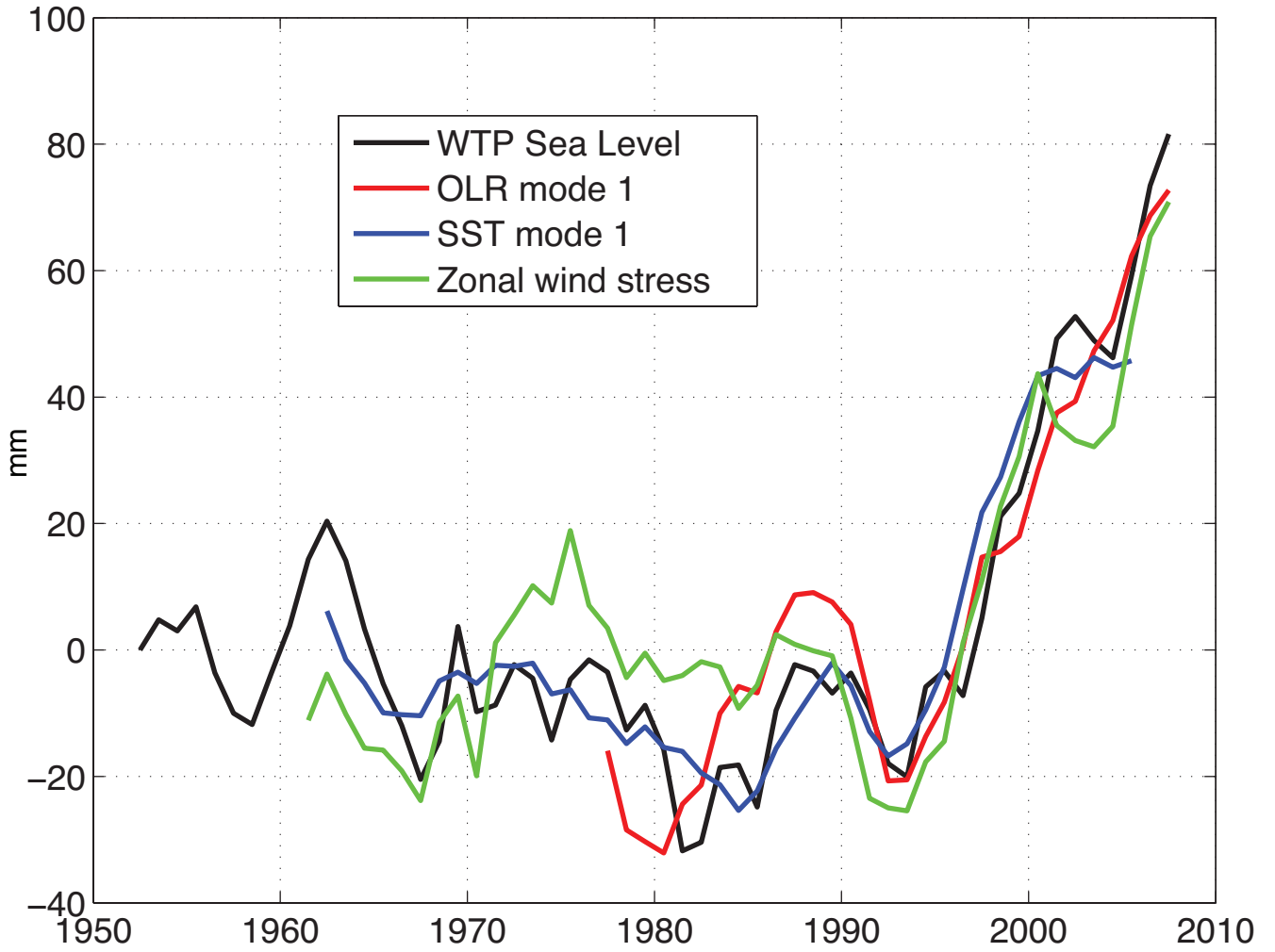


FIG. 15. Time series of WTP sea level, mode 1 OLR, mode 1 SST, and average zonal wind stress in the tropical Pacific all show a noticeable increase during the early 1990s. An offset and scale factor have been applied to OLR mode 1, SST mode 1, and mean zonal wind stress to match mean WTP sea level.